ARCHIVES

of

FOUNDRY ENGINEERING

Features of Cast Iron Smelting in Induction Crucible Furnaces

V. Grachev

A.N. Frumkin Institute of Physical Chemistry and Electrochemistry of the Russian Academy of Sciences, 29 Bldg 1,
Bolshaya Ordynka St., Suite # 104, 119017 Moscow, Russia
*Corresponding author. E-mail address: chernitsa@vernadsky.ru

Abstract

The article describes the trend towards increased use of induction crucible furnaces for cast iron smelting. The use of gas cupola's duplex process – induction crucible furnace – has been proved the effective direction of scientific and technical advance in the foundry industry. Gas cupolas and induction furnaces are used for cast iron smelting at the Penza Compressor Plant where in the 1960s the author developed and introduced gas cupolas for the first time in the world. In the article, the author represents the findings of the investigation on thermodynamics of crucible reduction of silicon, which is pivotal when choosing the technological mode for cast iron smelting in induction furnaces. The author proposes a new reaction crucible diagram with due account of both partial pressure and activity of the components involved into the process. For the first time ever, the electrochemical mechanism of a crucible reaction has been studied and the correctness of the proposed diagram has been confirmed.

1. Introduction

In the foundry, cast iron smelting is performed by gas cupolas and electric furnaces. Gas cupolas, natural gas-fired blast furnaces, were first developed and introduced with the participation of the author in Russia and Italy [1, 2]. The author has proved that smelting cast iron in a gas cupola allowed producing a wide range of high-quality castings [3]. Gas cupolas are still in operation at JSC Penzkompressormash.

The induction crucible furnaces have been used for smelting cast iron since the second half of 20th century. However, such type of smelting did not gain widespread acceptance. Gas cupola still remained the principal melting unit.

For cast iron smelting, the application of normal-frequency induction furnaces expands progressively. Since the late 1950s, smelting in electric furnaces, particularly in induction furnaces,

has been replacing cupola smelting in industrially developed countries. From 1963 to 1968, in the USA the number of operating electric furnaces reached 4,000 units. 70% of those were normal-frequency induction furnaces. During the last 6-7 years, the number of cupolas in the USA reduced almost by half, and the number of electric furnaces increased by 2.5 times. Replacement of cupolas by electric furnaces also takes place in Western Europe [2].

In the USSR, the first shop with normal-frequency induction furnaces instead of cupolas was launched in operation at Kaunas Cast Iron Foundry in 1963, almost alongside gas cupolas. At JSC Penzkompressormash, both gas cupolas and electric induction furnaces are used. Currently, its melting compartment is equipped with both gas cupolas and normal-frequency electric induction furnaces.

Smelting cast iron in induction furnaces has a set of features, which are discussed in the current paper. The main feature is that

melt carbon reduces silicon from the lining, significantly influencing the process.
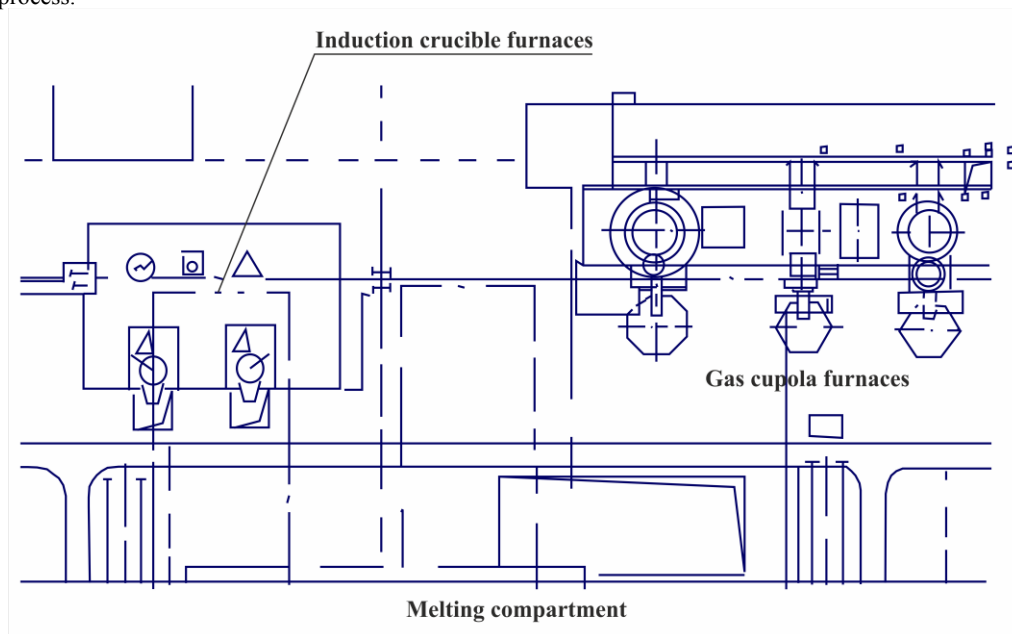

Fig. 1. Layout of the melting compartment, JSC Penzkompressormash foundry

2. Methods

The layout of the melting compartment is shown in Figure 1, images of gas cupolas and induction crucible furnaces are represented in Figure 2.

Fig. 2. Melting compartment, JSC Penzkompressormash

The electric induction furnace is a rather complicated batch-operated system (Figure 3).

The key advantage of the induction cast iron smelting compared to the cupola smelting lies in the possibility to control the process of cast iron superheating within a wide temperature-time range, perform a much deeper metallurgical treatment of the melt, accurately maintain chemical composition, and produce high quality cast iron. The advantages of such furnaces also include the possibility of remelting the non-briquetted cast iron turnings to 40% of metal charge, and sheet-iron scraps, which reduces consumption of pig iron and scrap. During smelting, the loss of Si and Mn, and the costs of the charge material are reduced, while the total loss does not exceed 2%. However, the maintenance costs increase (Table 1).
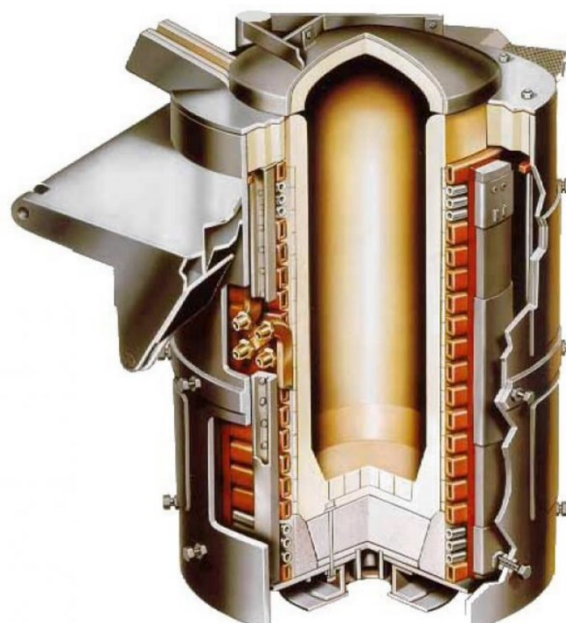

Fig. 3. Induction crucible furnace [4]

Table 1.
Cast iron smelting costs

Cost items	Costs, %		
	Coke cupola	Gas cupola	Induction furnace
Charge materials	60.71	56.08	46.62
Fuel (process energy)	10.50	2.09	14.01
Materials (except for the charge)	0.56	0.74	0.78
Electric furnace operation	0.31	0.12	0.76
Total	100%	100%	100%

Nevertheless, the induction furnaces are progressively replacing the cupolas (Figure 4) [5, 6, 7].
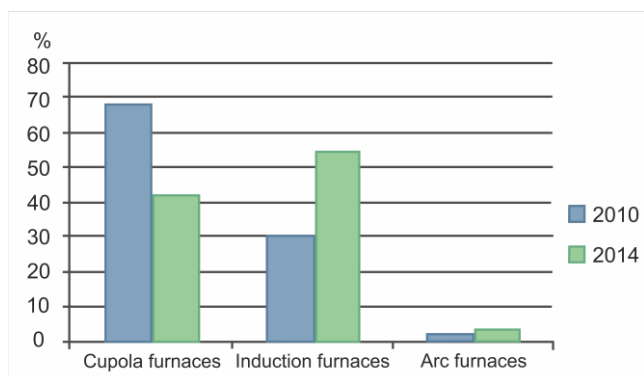

Fig. 4. Growth of cast iron production by induction furnaces in Russia

When smelting cast iron in induction furnaces, the content of S in the melt decreases drastically; this facilitates production of nodular cast iron. The hygiene and sanitary conditions of work significantly improve. Less harmful gases and dust is emitted, especially when compared to coke cupolas. Thus is particularly important for cities and residential areas, as the induction furnaces pollute the air much less than the cupolas that require bulky and expensive purification facilities. Specific consumption of refractories is also reduced: in case of an induction furnace, it amounts to 3 kg/t; in case of an acid-lined arc furnace, it is 17.6 kg/t; and in case of a gas cupola, it is 27 kg/t. It is lower in a gas cupola, as it can operate without repair for 2–3 weeks, and amounts to 13.6 kg/t. The atmospheric emission of dust from the gas cupola is 20 times lower than from the coke cupola, the CO content is 50 times lower, and the SO_2 content is 11 times lower. The use of gas cupolas in combination with induction furnaces is very promising.

3. Results

The melting compartment equipped with gas cupolas requires less capital investments during reconstruction of foundry shops and existing coke cupolas [5]. In the foundry industry, the use of induction electric furnaces for smelting cast iron has been progressively increasing.

One of the key features of smelting cast iron in induction furnaces is the occurrence of the crucible reaction:

$$\langle SiO_2 \rangle + [2C] = [Si] + \{2CO\}$$
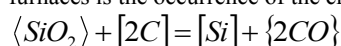
The equilibrium of this reaction plotted against the temperature is characterized by a diagram of equilibrium values of [Si] and [C] (referred to as Oelsen–Roesch–Orths diagram, Figure 5a). In Neumann–Dötsch study [8], this diagram is adjusted by value p_{CO}. At this, all authors considered that a_{SiO_2} = 1. However, the lining contains 60–65% of SiO_2, thus, a_{SiO_2} changes. $p_{CO} < 1$ may be important for vacuum melting, while in real-life induction melting conditions, the CO pressure reaches 2.5 atm and more.

In case of a crucible reaction, the actual values of a_{SiO_2} in the course of the crucible operation decrease from 1 to 0.6. The actual values of p_{CO}, in case of industrial furnaces, reach the values of 3 atm.

For the initial period of CO formation, when the radius of its incipient bubble is small, a significant resistance to crucible reaction is possible.

When analyzing the Neumann–Dötsch and our own data, equilibrium of the crucible reaction within the pressure range of p_{CO} = 1.5–3 atm and activity range of a_{SiO_2} = 0.6–1 should be considered. The adjustment of Oelsen–Roesch–Orths diagram carried out by Neumann and Dötsch concerned the activities a_C and a_{Si} with consideration of mutual influence thereof (Figure 5b) [8].

The author has studied how the activities and equilibrium concentrations of carbon and silicon are influenced by other elements usually contained in cast iron (Mn, S, P), and principal alloying elements (Cr, Ni, Al, Cu).

The calculation performed with consideration of influence coefficents ε_C^{Mn}, ε_C^{S}, etc., ε_C^{j} and ε_{Si}^{j} made it possible to determine corrections to equilibrium values of C and Si [3].

The changes in Si concentration equivalent to the change in activity are of such low significance ($\Delta Si_{Mn} + \Delta Si_S + \Delta Si_P \approx$ 0.1%) that it is possible to neglect them too, since this influence equals to only 5 °C change in equilibrium temperature [9].

The equilibrium of the crucible reaction may be significantly influenced by the alloying elements: large quantities of Cr inhibit the crucible reaction; the reaction is hastened by Ni, Cu and particularly large quantities of Al [3].

Figure 6 shows a nomographic chart plotted for real-life smelting conditions and allowing precise determination of the smelting mode.
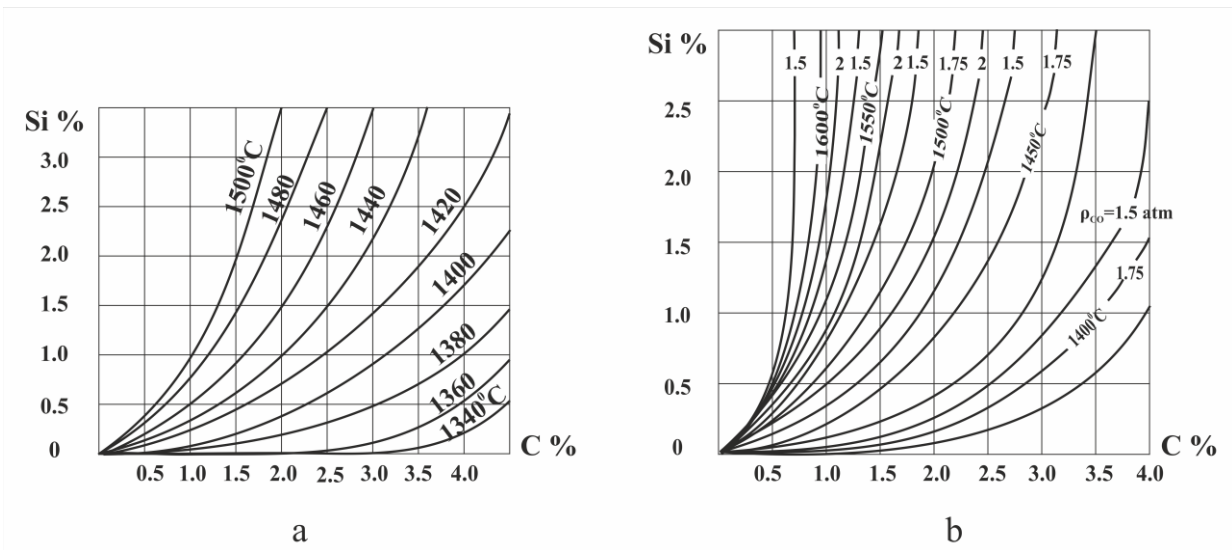
Fig. 5. Crucible reaction equilibrium diagram by: a) Oelsen–Roesch–Orths; b) Neumann and Dötsch
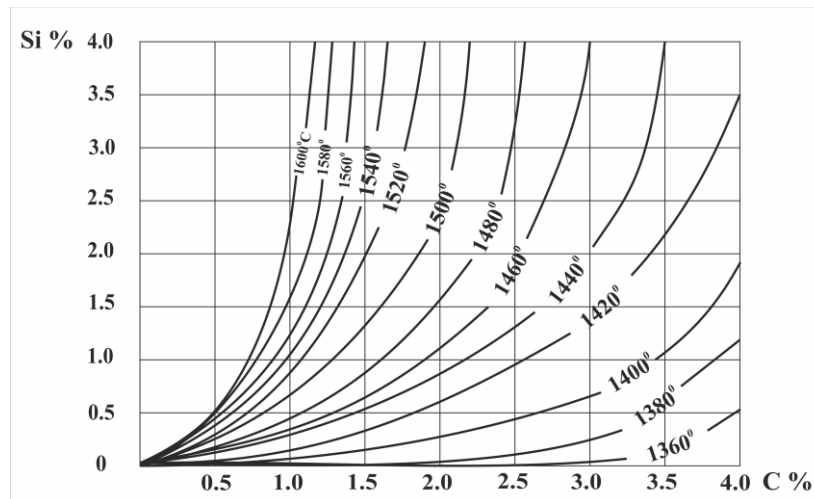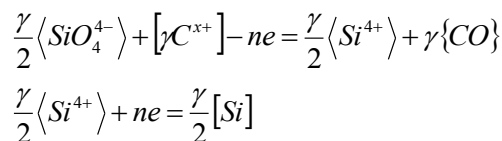

Fig. 6. Author's resultant diagram for the crucible reaction

The study of the crucible reaction mechanism has been conducted using samples of SiO_2 sintered with boric acid and placed into the melt of cast iron in the induction furnace. By passing currents of different magnitudes and polarities, it has been found that the crucible reaction may be hastened. The sample represented one of the electrodes. The other electrode was metal. Since the passage of electric current had a notable influence on the crucible reaction, we assume that between the electrodes there was an electrolyte. Then the mechanism of the crucible reaction may be represented as follows:

$$\frac{\gamma}{2}\langle SiO_4^{4-}\rangle + [\gamma C^{x+}] - ne = \frac{\gamma}{2}\langle Si^{4+}\rangle + \gamma\{CO\}$$

$$\frac{\gamma}{2}\langle Si^{4+}\rangle + ne = \frac{\gamma}{2}[Si]$$

This mechanism can be accepted only as a first approximation, since the structure high-silica layer is much more complicated than that of the ionic melt from SiO_4^{4-}.

The boundary layer of quartz lining consists of polyion complexes of various complexity, with inclusions of boric compounds and different kinds of impurities. The development of capillary and other phenomena results in a decrease in SiO_2 content to 60–70%.

According to Esin–Masson theory [2, 5, 6], the polymerization of silicon-oxygen anions occurs:

$$SiO_4^{4-} + SiO_4^{4-} = Si_2O_7^{6-} + O^{2-}$$

$$SiO_4^{4-} + SiO_7^{6-} = Si_3O_{10}^{8-} + O^{2-}$$
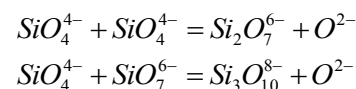
These reactions are characterized by polymerization constant K, and, in general case, the silicon ions have the form of

$Si_iO_{(3i+1-c)}^{2(i+1-c)}$, and the polymerization reaction may be represented as:

$$Si_iO_{(3i+1-c)}^{2(i+1-c)} + SiO_4^{4-} = Si_{i+1}O_{(3i+1-c)}^{2(i+1-c)-}$$
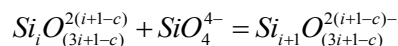
The calculations provided by O.A. Esin for different values of mole fraction of SiO₂ in silicate (N_{SiO_2}) have shown that even at $K = 0$ there were various kinds of complex anions present in the melt, which, according to Esin–Masson theory, is explained by the disproportionation reaction:
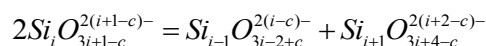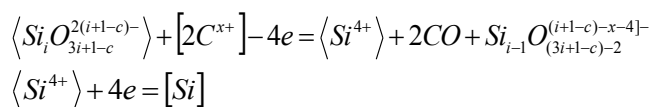
$$2Si_iO_{3i+1-c}^{2(i+1-c)-} = Si_{i-1}O_{3i-2+c}^{2(i-c)-} + Si_{i+1}O_{3i+4-c}^{2(i+2-c)-}$$

Table 2 shows the data on distribution of anions in melted silicates for values of N_{SiO_2} corresponding to 65.6% of SiO₂.

It is logical to assume that in the boundary layer of the lining, softened and glassified by sintering, the following process shall take place:

$$\left\langle Si_iO_{3i+1-c}^{2(i+1-c)-} \right\rangle + \left[2C^{x+} \right] - 4e = \left\langle Si^{4+} \right\rangle + 2CO + Si_{i-1}O_{(3i+1-c)-2}^{(i+1-c)-x-4]-}$$

$$\left\langle Si^{4+} \right\rangle + 4e = [Si]$$

Upon contacting with the Fe–Si–C–Mn melt, an interfacial exchange and creation of a double electric layer occurs. The electrochemical behavior of the crucible reaction makes is possible to determine the value of the protective potential that can inhibit, for example, the cathodic phase without intensifying the anodic phase.

Assuming that the crucible reaction consists of electrochemical actions at anode and cathode, a study of electrochemical phases of this reaction has been conducted using a standard potentiodynamic method and a P-5848 potentiostat, with the reference electrode placed in the boundary layer of the lining. The cell layout is presented in Figure 7. The obtained potentiodynamic curves are shown in Figure 8. On the

potentiodynamic curve, in case of Fe–3%C melt, there may be clearly seen two horizontal segments corresponding to the limit currents of the electrode processes (Figure 8a): Si⁴⁺ + 2e = Si²⁺ (segment I) and Si²⁺ + 2e = Si (segment II).

It was found that the first phase may be inhibited by an 800 mV voltage. On the curve corresponding to the high-silicon melt (Figure 8b), there may be observed certain oscillations (apparently, the formation of impurities) in a region close to the zero value of the current, which indicates that the reaction does not occur.

Whence, the author has obtained previously unknown data on the melt carbon interaction with the silicon oxide of the induction furnace lining under different thermodynamic conditions. The Oelsen–Roesch–Orths diagram was presented in a new form based on the real thermodynamic conditions of cast iron smelting in induction furnace. The correctness of the adjusted diagram was confirmed by electrochemical research.

The experimental data allowed calculating the empirical values of activation energy and obtaining the formula for determination of the protective potential:

$$\varepsilon_3 = \exp\left(\frac{1400}{T}\right)\left[\left(\frac{T}{23205}\ln\frac{P_{CO}\cdot P_{Si}}{a_C\cdot a_{SiO_2}} - 1.1\right)\right]$$

The possibility of protecting the lining from the crucible reaction was tested using a high-frequency induction furnace, wherein two alundum crucibles have been simultaneously lined, in one of which a protective current was applied to the inner lining, while in the other one no protective current was applied. The melt in the crucibles had the same composition. The crucible reaction behavior was judged by a change in the silicon content in the samples taken at regular intervals. It has been found that in the crucible, in which the protective current was not applied, the silicon content increased, and the carbon content decreased faster than in the crucible, in which the protective current was applied. It can be assumed that it was the electric current that influenced the process. However, this supposition needs further investigation.

Table 2.
Distribution of silicon-oxygen anions at various values of polymerization constant

| Mole fraction of slag content	Polymerization constant K value						
	0.17	1.0	2.0	5.0	10.0	20.0	50.0
SiO_2	0.7163	0.7163	0.7163	0.7163	0.7163	0.7163	0.7163
$Si_2O_4^{4-}$	0.116	0.107	0.057	0.021	0.014	0.003	0.00042
$Si_iO_{3i+1}^{2(i+1-c)-}$	0.034	0.0305	0.019	0.003	0.002	0.00016	0.000001
$Si_iO_{3i+1}^{2(i+1)-}$	0.167	0.15	0.072	0.024	0.016	0.003	0.00043
$Si_1O_{3i+1}^{2(i+1)-}$	0.137	0.114	0.068	0.022	0.019	0.0034	0.00044
$Si_iO_{3i}^{2i-}$ and ions at c > 1	0.695	0.736	0.837	0.961	0.968	0.997	0.991
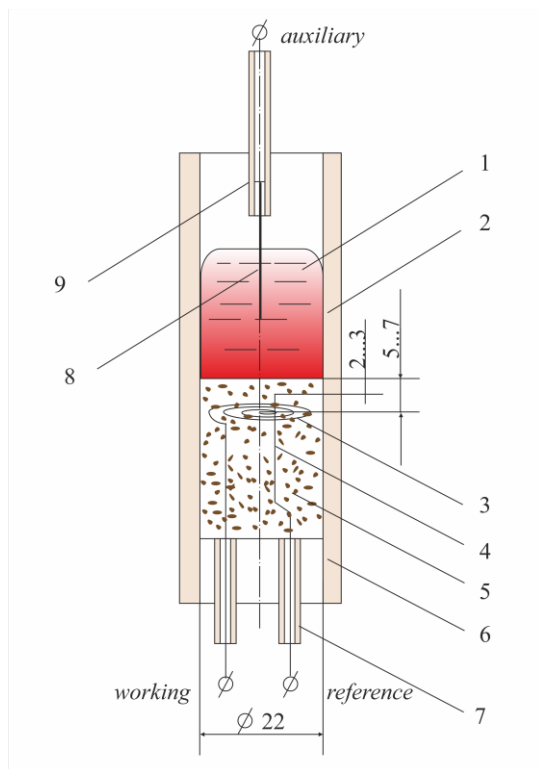
Fig. 7. The cell for studying the electrochemical processes in the boundary layer of the lining: 1 – cast iron melt, 2 – alundum casing, 3 – platinum working electrode, 4 – platinum reference electrode, 5 – lining made of SiO_2 with boric acid, 6 – plug made of Al_2O_3, 7 – insulating casings, 8 – auxiliary platinum electrode, 9 – insulation of auxiliary electrode
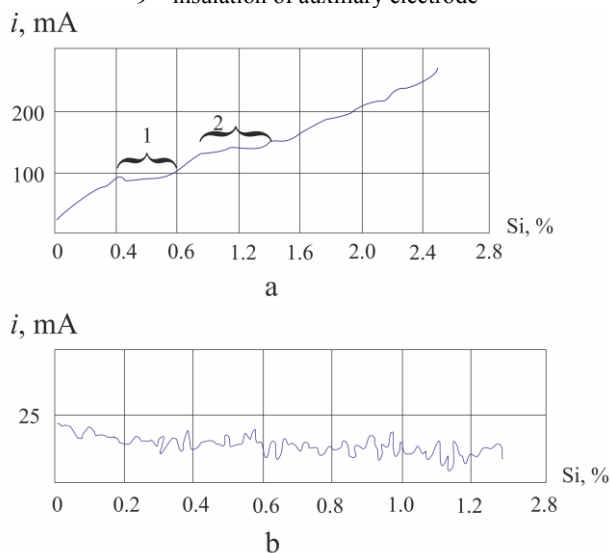

Fig. 8. Potentiodynamic curves representing Si content in cast iron (copied from the potentiostat diagrams): a. reaction occurs; b. reaction does not occur. Horizontal segments 1 and 2 correspond to the limit currents of the electrode processes: $1 - Si^{4+} + 2e = Si^{2+}$, $2 - Si^{2+} + 2e = Si$.

4. Conclusions

Cast iron smelting development trend attests to the fact that the use of induction crucible furnaces is expanding. Smelting in this type of furnaces has a set of features, which are primarily the reaction behavior for melt carbon interaction with silica of the lining according to the so-called crucible reaction.

The study of these features led to the following conclusions:

1. For the real conditions of cast iron smelting, the a_{SiO_2} activity decreases from 1 to 0.6, and the CO partial pressure differs from 1 and can reach 1.5–3.0 kg/cm^2. The author proposed a nomogram of crucible reaction equilibrium, which allows determining the melting mode for a variety of conditions.

2. The electrochemical mechanism of a crucible reaction has been ascertained empirically, as evidenced by the horizontal sections on potentiometric curves obtained in special electrochemical cells.

References

[1] Cherny, A.A., Marienbakh, L.M., Kurbatsky, I.L. et al. (1963). USSR certificate of authorship N 167613. Gas cupola. Moscow: State Committee for Inventions and Discoveries.

[2] Grachev, V.A. (2016). Development and application of gas cupolas in foundry production. *ARPN Journal of Engineering and Applied Sciences*. 11(23), 13790-13796.

[3] Grachev, V.A. (2016). *Physical and chemical basic principles of cast iron smelting*. Moscow: IPhKhiERAN.

[4] Fink, C. (2011, August 19). Long lining life and long coil life go hand-in-hand: For coreless *induction melting, an informed and effective maintenance approach will save thousands in repair and lining costs*. Retrieved November 30, 2016, from http://foundrymag.com/feature/long-lining-life-and-long-coil-life-go-hand-hand.

[5] Boldin, A.N. et al. (2010). *Engineering ecology of the foundry production*. Moscow: Mashinostroyeniye.

[6] Dibrov, I.A. (2014). State and prospects of the Russian foundry production. *UNIDO in Russia*. Special issue, 14-19.

[7] Dibrov, I.A. (2015). Development of the foundry engineering in Russia. *Liteishchik Rossii*. 8, 8-12.

[8] Neumann, F. & Dötsch, E. (1975). Thermodynamics of Fe-C-Si melts with particular emphasis on the oxidation behavior of carbon and silicon. *Giessereiforschung*, 27(1), 318-38.

[9] Grachev, V.A. (2016). Thermodynamics and mechanism of crucible reaction during cast iron smelting in induction furnaces. *Liteishchik Rossii*. 10, 11-15.